Evaluation of aqueous geochemistry of fluoride enriched groundwater: A case study of the Patan district, Gujarat, Western India

Pankaj Kumar, Chander Kumar Singh, Chitresh Saraswat, Binaya Mishra & Tejal Sharma

Published online: 03 May 2019.

Submit your article to this journal ↗

View Crossmark data ↗

Citing articles: 2 View citing articles ↗

Research Article

Evaluation of aqueous geochemistry of fluoride enriched groundwater: A case study of the Patan district, Gujarat, Western India

Pankaj Kumar [a,b,**], Chander Kumar Singh [c,d,*], Chitresh Saraswat [a], Binaya Mishra [a], Tejal Sharma [b]

[a] *United Nations University, Institute for the Advanced Study of Sustainability, Tokyo, Japan*
[b] *Institute of Science and Technology for Advance Studies and Research (ISTAR), Gujarat, India*
[c] *School of Environmental Science, Jawaharlal Nehru University, New Delhi 110067, India*
[d] *Dept. of Energy and Environment, TERI University, New Delhi 110070, India*

Abstract

High fluoride (F^-) groundwater causes fluorosis which might at severe stages lead to deformation of bones, bilateral lameness. The concentration of F^- ranged from 0.4 to 4.8 mg/L. This study suggests that high HCO_3^- and Na^+ in alkaline medium along with water–rock interaction plays important role in enrichment of F^- in groundwater. $Na-HCO_3$ is the dominant water type followed by $Ca-HCO_3$ suggesting dominance of Na^+, Ca^{2+} and HCO_3^- ions in groundwater. Factor analysis of water quality parameters suggests that four principal components account for 74.66% of total variance in the dataset. Factor 1 shows higher positive loading for pH, HCO_3^- negative loading for F^-, Ca^{2+}, SO_4^{2-} depicting ion-exchange and HCO_3 dominant water type responsible for F enrichment in groundwater.

Saturation index for selected minerals suggests that most of the samples are oversaturated with calcite and undersaturated with fluorite. Calcite precipitation leads to the removal of Ca^{2+} from solution thus allowing more fluorite to dissolve. These released Ca^{2+} ions combine with CO_3^{2-} ions to further enhance the precipitation of $CaCO_3$.
© 2017 National Water Research Center. Production and hosting by Elsevier B.V. This is an open access article under the CC BY-NC-ND license (http://creativecommons.org/licenses/by-nc-nd/4.0/).

Keywords: Fluoride; Rock–water interaction; Saturation index; Groundwater

1. Introduction

Fluoride is a normal constituent of natural water. Globally the health of millions of people is threatened by endemic fluorosis because of consumption of groundwater polluted with F^- (UNICEF, 2008). At the global scale, high concentrations of F^- (i.e. >1.5 mg/L) are found in groundwater in China, Syria, Jordan, Ethiopia, Sudan, Tanzania, Kenya

and Uganda (Ando et al., 2001). In the case of India, groundwater contamination with F^- is well reported at numerous places in the States of Andhra Pradesh, Gujarat, Karnataka, Madhya Pradesh, Rajasthan, Chhattisgarh, Haryana, Orissa, Punjab, Haryana, Uttar Pradesh West Bengal, Bihar, Delhi, Jharkhand, Maharashtra, and Assam (Keshari and Dhiman, 2001; Jacks et al., 2005; CGWB, 2010). Occurrence of F^- in groundwater at different parts of Rajasthan is extensively documented by the scientific community (Madhavan and Subramanian, 2002; Singh et al., 2012; Hussain et al., 2012). In case of Gujarat, Mehsana district is well reported for factors responsible for F^- pollution in groundwater by Dhiman and Keshari (2006), however it is still poorly reported for many administrative units of Gujarat where people are suffering from fluorosis.

Because of its high reactivity, fluorine normally, exists in the form of F^- in natural waters (Leung and Hrudey, 1985). Although geological sources contribute to the occurrence of F^- in water, the major contribution comes from geological sources and conditions in hydro-geoenvironment such as the porosity and acidity of the soil and rocks, temperature i.e. semi-arid climate, the action of other chemicals, advanced stage of groundwater development and the depth of wells (Johnson et al., 2008; Ranjan et al., 2013). F^- in groundwater is mainly derived from the weathering and leaching of rocks commonly containing minerals such as fluorite, fluorapatite, cryolite, amphibole, muscovite, biotite, (Carrillo-Rivera et al., 2002; Avtar et al., 2013). Due to a presumed lack of geochemical controls F^- concentrations vary by more than an order of magnitude, the F^- concentrations in groundwater range from well under 1.0 mg/L to more than 35.0 mg/L (IPCS, 1984).

F^- helps in the normal mineralization of bones and formation of dental enamel (Cao et al., 2000). The total daily intake of F^- from food is about 0.2–0.5 mg which is about only 10–15% of the required dose and hence humans are dependent on groundwater to fulfill this deficit (Boyle and Chagnon, 1995). The desirable safe limit of F^- in drinking water is 1.5 mg/L (WHO, 1993). In case of daily intake of F^- is low (i.e. <0.5 mg/L), various health issues may occur viz. dental caries, lack of formation of dental enamel and deficiency of mineralization of bones, especially affecting the children (Mondal et al., 2009). When F^- is consumed in the range of 1.5–2.0 mg/L, dental fluorosis or dental mottling may occur which is characterized by brown or black opaque patches on the enamel/tooth surface (Kharb and Susheela, 1994). When long term intake of F^- exceeds 3.0 mg/L, skeletal fluorosis may occur characterized by deformation of bones (Goldman et al., 1991). Other than the above mentioned health issues, excessive intake of F^- may lead to too much thirst, skin rashes, muscle fibre degeneration, blood cells deformation, gastrointestinal problems, urinary tract malfunctioning, and overall reduced immunity (Meenakshi and Maheshwari, 2006; Singh et al., 2011a).

With the above background, this work strives to evaluate the geochemistry of groundwater with special focus on geochemical processes controlling F^- mobilization in Patan district, Gujarat, India.

2. Study area

The study area (Patan district) showing groundwater sampling location and F^- safe and unsafe water is given in Fig. 1. The study area is located between $23°\ 55'$ and $24°\ 41'$ N and $71°\ 31'$ and $72°\ 20'$ E. Patan is situated in the northern part of Gujarat on the bank of the Saraswati River. The study area is bound on the North West by Rann of Kutch, on the North by Banaskantha district and in South East sharing a common border with Patan district. The total geographical area of the district is about 5740 km^2. The climate of the area is warm, sub-humid and sub-tropical. May is generally the hottest month and January, the coldest. The region has a minimum temperature as low as $5\ °C–10\ °C$ and a maximum temperature as high as $40\ °C–48\ °C$. The mean annual rainfall is 765 mm, 95% of which is received due to Southwest monsoon, from June to mid-September. The topography varies from plains to low hilly ranges, with elevation gradients of 10 m–190 m above mean sea level. Patan district is a part of Gujarat plain and is sub-divided into three sub-micro regions, namely Western Sandy Waste, Central Alluvial Plain and Mahesana Low Land. Western Sandy Waste region has low relief in comparison to other regions of the district. Saraswati is the main river of the region, flows from north-east to south-west direction and ultimately submerges into the Little Rann of Kachchh. Geologically all the three divisions are part of wind-blown sand and almost the entire region has alluvium deposition and the clay layer thickness is 4 m. The region has Orthids-Aquepts, Orthids-Psamments and Ochrepts-Psamments types of soils. Central Alluvial Plain region slopes towards west. Thus, all the rivers Banas, Saraswati, Rupen and their tributaries which form the drainage pattern of this region, flow towards westerly direction. The Mahesana Low Land is flat and of sandy plain. Geological origin of the entire Patan landscape implies that it is generated due to prolonged alluvial action in Quaternary period. Since the area is geotectonically a graben of early Tertiary period, it provides a room
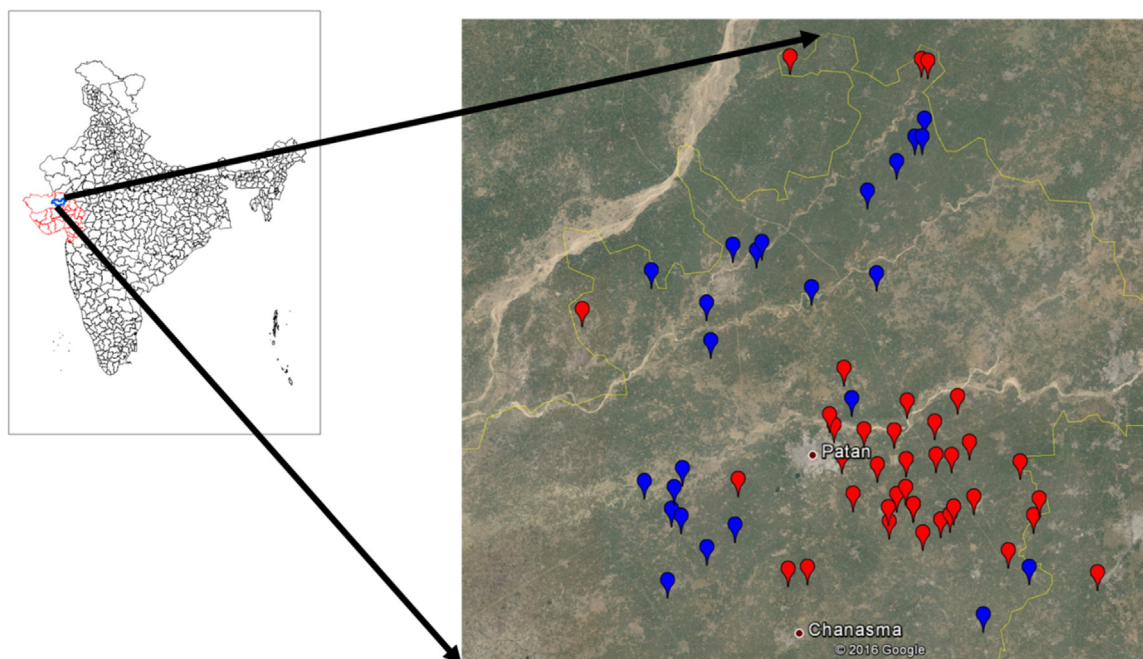
Fig. 1. Study area map showing (a) groundwater sampling location, and fluoride safe (blue) and unsafe water (red).

for large scale alluvial deposition through major river systems from the Aravallis. Geologically, whole study area is blanketed with thick alluvium. Highly weathered granites lead to the formation of clay. Over the granites lie the Himmatnagar formation, comprising sandstone, conglomerate and shale. These formations are also highly weathered. Geologically and mineralogically, this area is dominated by pegmatites, amphibolites, quartz, feldspar, china clay and fire clay. Soil present in this region is mainly classified into saline-alkali soil, calcareous sandy loams, calcareous sandy soil, non-calcic brown soils and non-calcic red-brown soils (UNDP/CGWB, 1976). Hydrogeologically, the area has unconsolidated aquifers with very high yield ranging from 1000 to 3000 lpm.

3. Sampling, analytical techniques and multivariate statistical analysis

3.1. Sampling

The health survey carried out by the local municipality, reported that the people in seven sub-divisions of Patan District of Gujarat, are suffering from both dental and skeletal fluorosis. Henceforth, a random sampling approach was adopted to collect a total of sixty two groundwater samples with an idea to create a hydrochemical mapping of different water resources in the study area. Water samples were collected in clean polypropylene bottles from open wells, dug wells, hand pumps and tube wells at varying depths. At the time of sampling, the source was purged for 5 min and bottles were thoroughly rinsed 2–3 times with sample water to be collected.

3.2. Analytical techniques

The sampling locations were recorded using the Global Positioning System (GPS III, Garmin). On-site measurements of the electrical conductivity (EC) and pH were made using an in-line flow cell to ensure the exclusion of atmospheric contamination and to minimize the fluctuations in space and time. The portable Orion Thermo water analyzing kit (Model Beverly, MA, 01915) with a precision of 1% was used for all on-site measurements. Two samples were collected from each location (average of which is presented in the result section) and filtered using 0.2 μm Millipore membrane filters made up of biologically inert mixtures of cellulose acetate & cellulose nitrate. The samples collected for cation analysis were acidified using 1% HNO_3 to stabilize trace metals (pH ∼ 2), while samples collected for nitrate

were acidified with H_3BO_3. Samples were brought to laboratory in an ice chest and stored at 4 °C. On the same day, alkalinity was analyzed by Gran titration using 0.05 N HCl solutions. The concentration of HCO_3^- was analyzed by acid titration (using Metrohm Multi-Dosimat) while other anions Cl^-, NO_3^-, SO_4^{2-} and F^- were analyzed by DIONEX ICS-90 ion chromatograph with an error of <2% using duplicates. Major cations were determined with an atomic absorption spectrometer (Thermo Fisher) with a precision of <2% using duplicates. For major ions, analytical precision was checked by normalized inorganic charge balance (NICB) (Kumar et al., 2010). This is defined as $[(Tz+ - Tz-)/(Tz+ + Tz-)]$ and represents the fractional difference between total cations and anions. The observed charge balance supports the quality of the data points, which is better than ±5%, and generally the charge imbalance was in favor of positive charge. This imbalance in charge may be attributed to the failure to analyze organic matter, which is mainly produced by biological activities (Huh et al., 1998).

3.3. Multivariate statistical analysis (factor analysis FA and principal component analysis PCA)

Chemometric analysis of the hydro-chemical data set was performed through correlation and principal component analysis using the xl-stat (addon module of Microsoft Excel). Factor analysis was applied on the experimental data standardized through z-scale transformation in order to avoid misclassification due to wide differences in data dimensionality (Reghunath et al., 2002; Liu et al., 2003; Singh et al., 2011b). Standardization tends to minimize the influence of difference of variance between variables and eliminates the influence of different units of measurement and renders the data dimensionless. PCA is an independent method which captures the variability of the dataset. It is a pattern recognition technique that attempts to explain the variation of large set of intercorrelated variables and transform them into smaller set of uncorrelated variables. Principal components (PCs) provide information on most meaningful parameters, which describes all data and reduces dataset with minimum loss of original information. PCs are produced by multiplying original correlated variables with eigenvector. PC loadings are the eigenvectors of covariance or correlation matrix, and the scores are individual transformed observations. PCs show the correlations present in the dataset. PCA was performed using varimax rotation method with Kaiser normalization. PCs with eigen value >1 are taken into account to infer the information on dominant geochemical processes in the region.

3.4. Geochemical modelling

In order to understand the origin of groundwater mineralization and the processes responsible for F^- enrichment in groundwater in the study area, saturation index (SI) was calculated using PHREEQC code (Parkhurst and Appelo, 1999). Saturation indices indicate the thermodynamic tendency of minerals to dissolve or precipitate. The changes in saturation state are useful to distinguish different stages of hydrochemical evolution and help to identify which geochemical reactions are important in controlling water chemistry (Coetsiers and Walraevens, 2006). The saturation index of a mineral can be obtained using Eq. (1) (Garrels and Mackenzie, 1971):

$$SI = log_{10}\left(K_{IAP}/K_{SP}\right). \tag{1}$$

where, SI is the saturation index, K_{IAP} is the ion activity product of particular solid phase and K_{SP} is the solubility product of the phase. Based on the value of the SI, the saturation states are recognized as saturation (equilibrium; $SI = 0$), under saturation (dissolution; $SI < 0$) and oversaturation (precipitation; $SI > 0$).

4. Results

4.1. Water quality variables distribution

The statistical summary of physico-chemical parameters for groundwater samples analyzed is presented in Table 1. The values of pH ranged from 7.0 to 8.2 with an average value of 7.5 signifying slightly alkaline conditions being dominant within groundwater system in the region. The electrical conductivity (EC) in the water samples ranged from 460 μs/cm to 3160.4 μs/cm with an average value of 1420.2 μs/cm. Higher order of EC values indicates high concentration of dissolved solids and/or high ionic strength of the groundwater, local variation in soil type, multiple aquifer system, and salt accumulations due to increased evaporation. Among cations, the dominance was found to be in the order $Na^+ > Ca^{2+} > Mg^{2+} > K^+$ and the contribution ratio was 47.3%, 24.4%, 21.2% and 7.1% respectively. Anions

Table 1
Hydro-geochemical parameters of groundwater analyzed from the study area.

ID	Depth	pH	EC	Alkanity	Ca^{2+}	Mg^{2+}	Na^+	K^+	HCO_3^-	SO_4^{2-}	Cl^-	F^-	NO_3^-
P1	700	7.30	3160	15.87	34.00	42.00	133.16	2.19	595.36	97.00	72.00	2.00	32.77
P2	760	7.24	1143	15.73	30.00	28.00	83.51	2.91	400.16	61.00	96.00	2.11	21.60
P3	500	7.08	954	15.39	176.00	99.00	82.38	2.91	429.44	65.00	142.00	1.75	297.54
P4	850	7.64	931	16.60	38.00	27.00	60.94	4.37	302.56	103.00	86.00	2.24	6.33
P5	550	7.72	1054	16.78	27.00	30.00	108.33	3.64	405.04	49.00	86.00	1.23	46.55
P6	400	7.21	2500	15.67	55.00	45.00	62.07	4.37	497.76	60.00	72.00	1.08	71.50
P7	665	7.16	1514	15.56	12.00	20.00	88.02	12.39	497.76	26.00	96.00	1.44	53.63
P8	780	7.52	1786	16.34	21.00	20.00	83.51	2.19	614.88	42.00	44.00	2.50	38.54
P9	650	7.44	1917	16.17	21.00	26.00	54.17	3.64	366.00	86.00	127.00	1.79	25.51
P10	800	7.04	2391	15.30	46.00	38.00	106.08	2.19	531.92	40.00	60.00	1.33	59.58
P11	1000	7.22	1434	15.69	37.00	30.00	82.38	2.91	409.92	88.00	50.00	1.71	21.79
P12	1000	7.16	1023	15.56	30.00	20.00	72.22	2.91	400.16	32.00	160.00	1.76	18.62
P13	850	7.08	1403	15.39	40.00	34.00	83.51	4.37	385.52	43.00	78.00	1.60	19.36
P14	650	7.18	1991	15.60	43.00	24.00	93.66	2.91	502.64	85.00	72.00	1.73	27.93
P15	1100	7.78	1194	16.91	40.00	5.00	69.97	5.10	405.04	69.00	32.00	3.86	23.46
P16	740	7.58	717	16.47	34.00	11.00	63.19	2.91	326.96	27.00	120.00	2.67	13.96
P17	830	7.82	1509	17.00	42.00	33.00	62.07	5.83	419.68	141.00	56.00	2.92	23.65
P18	520	7.05	1691	15.32	72.00	73.00	62.07	3.64	536.80	43.00	336.00	1.04	106.32
P19	250	7.05	466	15.32	38.00	17.00	81.25	3.64	200.08	48.00	56.00	0.40	6.89
P20	800	7.15	1334	15.54	32.00	16.00	88.02	2.19	400.16	38.00	328.00	1.42	24.95
P21	560	7.26	1329	15.78	42.00	25.00	82.38	8.74	419.68	56.00	264.00	1.24	38.17
P22	900	7.14	1397	15.52	40.00	28.00	82.38	2.19	468.48	48.00	60.00	1.50	44.50
P23	280	7.06	1129	15.34	21.00	13.00	80.12	2.19	478.24	95.00	136.00	0.79	43.20
P24	900	7.55	1591	16.41	32.00	27.00	29.34	3.64	446.52	55.00	102.00	2.00	46.92
P25	310	7.01	460	15.23	35.00	19.00	86.89	2.19	190.32	28.00	48.00	0.40	6.70
P26	820	7.68	906	16.69	19.00	12.00	75.61	2.19	214.72	21.00	200.00	2.65	27.93
P27	880	8.00	3053	17.39	87.50	92.50	170.19	2.25	152.50	63.07	182.86	3.88	1.15
P28	950	8.05	1430	17.49	87.25	27.75	106.73	3.00	152.05	69.01	55.98	4.02	0.53
P29	470	7.43	1194	16.15	87.05	17.95	105.29	3.00	152.25	80.01	35.45	2.90	0.57
P30	975	7.86	1165	17.08	75.00	25.00	77.88	4.50	152.75	77.88	77.99	4.32	0.51
P31	585	7.61	1319	16.54	87.50	12.50	138.46	3.75	152.30	117.91	77.99	2.94	0.49
P32	625	7.20	3128	15.65	162.50	112.50	79.33	4.50	152.50	183.06	319.05	2.42	0.75
P33	865	7.78	1895	16.91	62.50	17.50	112.50	12.75	152.42	104.28	113.44	4.00	2.92
P34	970	7.85	2234	17.06	45.00	15.00	106.73	2.25	305.00	98.32	106.35	4.23	1.06
P35	590	7.45	2399	16.19	40.00	15.25	69.23	3.75	152.50	107.27	49.63	2.25	0.56
P36	810	7.74	2992	16.82	100.00	55.00	135.58	2.25	152.25	77.95	283.60	3.10	0.50
P37	750	7.68	1794	16.69	112.50	42.50	105.29	3.00	305.00	130.68	134.71	3.67	0.57
P38	925	7.40	1280	16.08	75.00	25.00	92.31	3.00	305.25	42.18	85.08	3.71	0.81
P39	850	7.40	1755	16.08	112.25	37.75	106.73	4.50	152.50	54.24	141.80	3.65	0.55
P40	700	7.90	2491	17.17	75.00	40.00	119.71	3.00	305.00	10.71	177.25	4.19	0.60
P41	1000	7.90	1494	17.17	62.50	37.50	89.42	5.25	305.50	48.34	106.35	4.75	0.67
P42	1050	7.45	897	16.19	62.25	7.75	80.77	3.00	152.50	126.00	63.81	4.27	0.60
P43	1000	7.80	1887	16.95	125.00	30.00	79.33	6.00	152.25	74.54	134.71	4.44	0.64
P44	270	7.20	2116	15.65	112.50	77.50	79.33	3.75	152.50	115.78	77.99	0.39	0.72
P45	940	7.20	583	15.65	125.00	45.00	103.85	3.75	305.00	118.76	155.98	3.56	2.54
P46	800	7.20	1669	15.65	62.50	27.50	112.50	2.25	305.50	108.12	148.89	3.90	3.18
P47	720	7.00	1662	15.21	112.50	52.50	105.29	9.00	152.50	54.75	127.62	3.10	0.55
P48	900	7.30	1748	15.87	87.50	47.50	105.29	2.25	402.25	138.78	120.53	3.71	0.85
P49	665	7.50	1412	16.30	37.50	47.25	102.40	2.25	341.55	131.11	77.99	2.92	0.72
P50	200	7.20	1991	15.65	62.50	17.50	37.50	3.75	361.22	62.13	21.27	0.54	0.56
P51	900	7.70	576	16.73	112.50	97.50	111.06	2.25	282.05	140.05	184.34	3.36	0.63
P52	1100	8.10	1133	17.60	37.50	12.50	96.63	2.25	352.50	92.36	77.99	4.23	0.60
P53	1000	8.20	2638	17.82	62.50	12.50	106.73	3.75	222.00	171.74	120.53	4.63	1.66
P54	800	7.90	1995	17.17	137.50	22.50	121.15	19.50	161.00	188.12	155.98	4.53	0.77
P55	800	7.82	2382	17.00	62.50	12.50	37.50	4.50	248.80	119.62	21.27	4.40	0.58

Table 1 (*Continued*)

ID	Depth	pH	EC	Alkanity	Ca^{2+}	Mg^{2+}	Na^+	K^+	HCO_3^-	SO_4^{2-}	Cl^-	F^-	NO_3^-
P56	675	8.00	1731	17.39	137.50	162.50	137.02	42.75	97.60	202.33	191.43	3.93	8.90
P57	890	7.71	2949	16.76	87.50	77.50	154.33	3.00	197.60	27.93	69.42	4.32	1.86
P58	775	7.94	2711	17.26	87.50	72.50	141.35	3.75	61.00	216.98	205.61	4.48	0.32
P59	850	7.64	1755	16.60	112.25	37.75	106.73	4.50	252.50	54.24	141.80	3.65	0.55
P60	840	7.79	2491	16.93	75.00	40.00	119.71	3.00	305.00	170.71	177.25	4.19	0.60
P61	790	8.10	1494	17.60	62.50	37.50	89.42	5.25	305.50	118.34	106.35	4.75	0.67
P62	975	8.20	897	17.82	62.25	7.75	80.77	3.00	152.50	126.00	63.81	4.27	0.60

Table 2
Classification of groundwater samples based on Fluoride concentration and associated risk.

Classification	F^- (mg/L)	Associated risk	No. of samples found in this range	Value in percentage
Safe	<1.5	Within permissible limit (WHO, 1993)	12	19.4
Low risk	1.5–3.0	Dental fluorosis	20	32.2
High risk	3.0–5.0	Dental and mild skeletal fluorosis	30	48.4
Very high risk	>5.0	Severe skeletal fluorosis	Nil	Nil
Total			62	100

dominance followed the order $HCO_3^- > Cl^- > SO_4^{2-} > NO_3^- > F^-$ and their contribution ratio was 37.6%, 31.8%, 11.2%, 9.4% and 3.3% respectively. Average value of depth for sampling wells is 758.8 ft which shows water table is depleted in nature a typical signature of arid/semi-arid.

4.2. General hydro-geochemistry and F^- contamination

F^- concentration in the groundwater samples ranged from 0.4 to 4.8 mg/L with an average value of 2.9 mg/L. A brief classification of groundwater samples based on F^- concentration and associated risk in the study area is shown in Table 2. It was found that that only 19.4% of water samples contained F^- concentration less than the permissible limit given by WHO, thus safe to consume for drinking or cooking purpose. Rest of the water samples fall into the category of low risk (32.2%, F^- 1.5–2.9 mg/L) or high risk (48.4%, F^- 3.0–5.0 mg/L) category. The highest concentration recorded was 4.8 mg/L, therefore no sample is found within the category of very high risk.

Scatter plot showing the relation between F^- versus well depth and various water quality parameters viz. pH, alkalinity, Ca^{2+} and NO_3^- (Fig. 2) can help decipher the mechanism for F^- enrichment in the aquifers. The vertical distribution profile of F^- (Fig. 2a) clearly indicates a general increase in concentration with screen or strainer depth of sampling wells). With alkaline pH, F^- concentration is also found to increase for most of the water samples, which has been commonly observed in different parts of the world.

The relationship between F^- and total alkalinity is shown in Fig. 2c, which reveals a strong linear association (with correlation coefficient (r) = 0.89).

In the scatter plot (Fig. 2d), an inverse relation is found between F^- and Ca^{2+} (with correlation coefficient r = −0.34). In contrast to this, inverse relation between F^- and nitrate (with correlation coefficient r = −0.19) is shown in Fig. 2e. Most of the data points are confined to low concentration of nitrate. Further, the ratio of Na^+/Ca^{2+} (average value of 4.08/3.66 meq/L), it is found that most of the samples have a value greater than one (1.11) indicating low calcium activity. It is also well reported that a high concentration of Na^+ favors the dissolution of F^- bearing minerals in an alkaline medium (Shaji et al., 2007). Ion exchange between Na^+ and Ca^{2+} due to the movement of groundwater in the weathering zone may also result in high F^- associated with high Na^+ and low Ca^{2+} concentration because of the precipitation of the CaF_2.

4.3. Hydrochemical facies

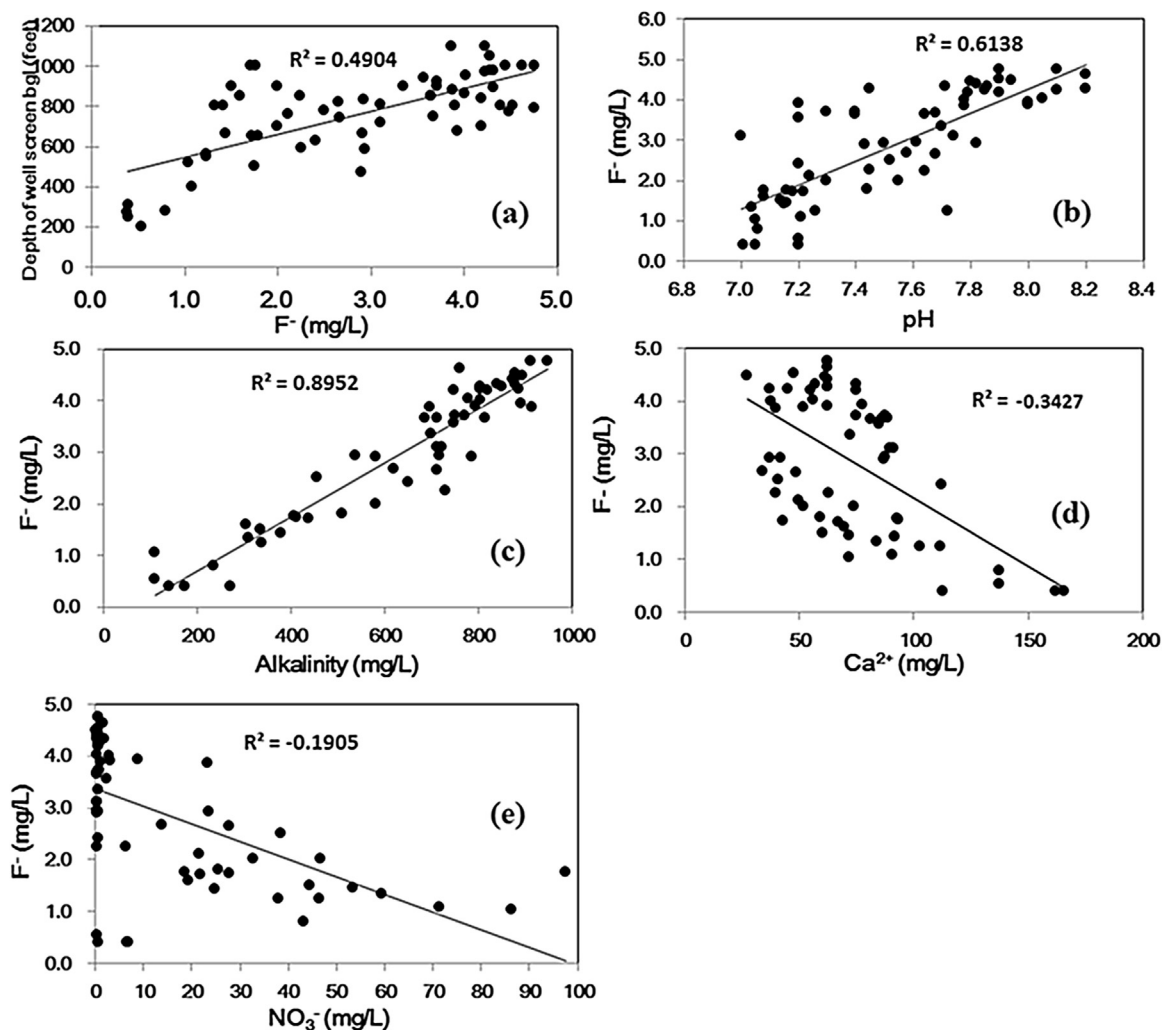Hydrochemical facies of groundwater identifies the chemical characteristic of water in the aquifer system.

Fig. 2. Scatter plot of F^- versus (a) depth, (b) pH, (c) alkalinity, (d) Ca^{2+} and (e) NO_3^-.

These water facies reflects the chemical process between the mineral and water within the lithological context. The Piper trilinear plot include two triangles, one of which represents anion and the other the cations. The cation and anion fields are represented together in a diamond-shaped field. This diamond shape field represents different water types belonging to any genetically related system (Mallick, 2017).

Piper trilinear equivalence diagram is one of the widely used graphical charts to represent hydrochemical data (using all major ions) into different water facies (Piper, 1994). Based on the piper diagram (Fig. 3), groundwater samples were classified in nine geochemical facies. $Na-HCO_3$ type is most dominating one (52%) followed by $Ca-HCO_3$ (13%), Na-Cl (12%), Mg-Cl (8%), $Mg-HCO_3$ (6%), Ca-Cl (6%) and $Na-SO_4$ (3%). Ion exchange, dissolution of calcite, semiarid climate, alkaline condition and weathering are responsible for high concentration of Na^+, Ca^{2+} and HCO_3^-. HCO_3^- dominance in water type suggests dissolution of calcite minerals which favors the enrichment of F in the aquifer.

4.4. Geochemical modeling

Saturation indices indicate the thermodynamic tendency of minerals to dissolve or precipitate. Undersaturation reflects the character of water from a formation with insufficient amount of the mineral for solution or with short residence time. On the other hand, oversaturation depicts that the groundwater discharging from an aquifer containing
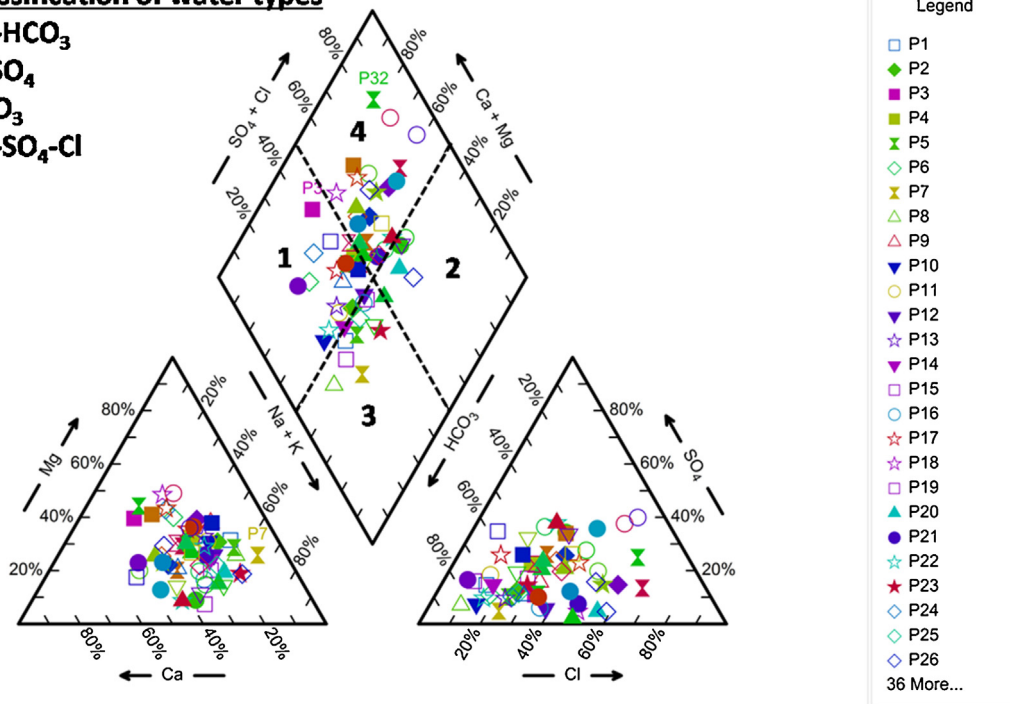
Fig. 3. Piper diagram showing hydrochemical facies in groundwater samples.

sufficient amount of the mineral with long residence time to reach equilibrium. Different plots showing saturation indexes for six selected minerals and plot exclusively of SI (Fluorite) versus SI (Calcite) to elucidate the process responsible for F^- enrichment is shown in Fig. 4a and b respectively.

From Fig. 4a, the positive values of the calculated SI with respect to aragonite, calcite and dolomite for majority of the water samples suggest their oversaturation with respect to these minerals. On the other hand, negative values of the calculated SI with respect to anhydrite, fluorite and hydroxyapatite for almost all water samples (except few one in case of fluorite) suggest undersaturation.

Undersaturation with respect of fluorite can be further explained by a scatter plot between calcite and fluorite (Fig. 4b). It is observed (Fig. 4b) that most of the samples are oversaturated with respect to calcite, whereas most of the water samples are undersaturated with respect to fluorite.

4.5. Multivariate analysis

Factor analysis of physio-chemical parameters of the groundwater samples suggests that four components account for 74.66% of total variance in the composition of groundwater in the study area (Table 3). 29.65% of variance is explained by PC1, 19.25% by PC2, 16.71% by PC3, and 9.04% by PC4. Component loadings which had values greater than 0.5 were considered for interpretation. Factor 1 has higher positive loading for pH, HCO_3^-, Cl^-, and alkalinity and higher negative loading for F^-, Ca^{2+}, SO_4^{2-} (Table 4). It shows that at a higher pH ionic exchange occurs between F^- and OH^- ions (from minerals like illite, muscovite, amphiboles and mica), resulting in an increase of F^- concentration in groundwater. The higher loading for HCO_3^-, which is also supported by the fact that most of the water facies belong to HCO_3^- type, favors the release of F into groundwater. At higher pH ionic exchange occurs between F^- and OH^- ions (illite, mica and amphiboles) resulting in increase of F^- ion concentration in groundwater. The presence of high HCO_3^-, Na^+ and pH favors the release of F^- from aquifer matrix into groundwater.

Factor 2 has a higher positive loading of TDS, EC, Na^+ and SO_4^{2-} (Table 4). It suggests the soil mineralization as well as anthropogenic sources such as agriculture is influencing the groundwater environment. Relatively less loading
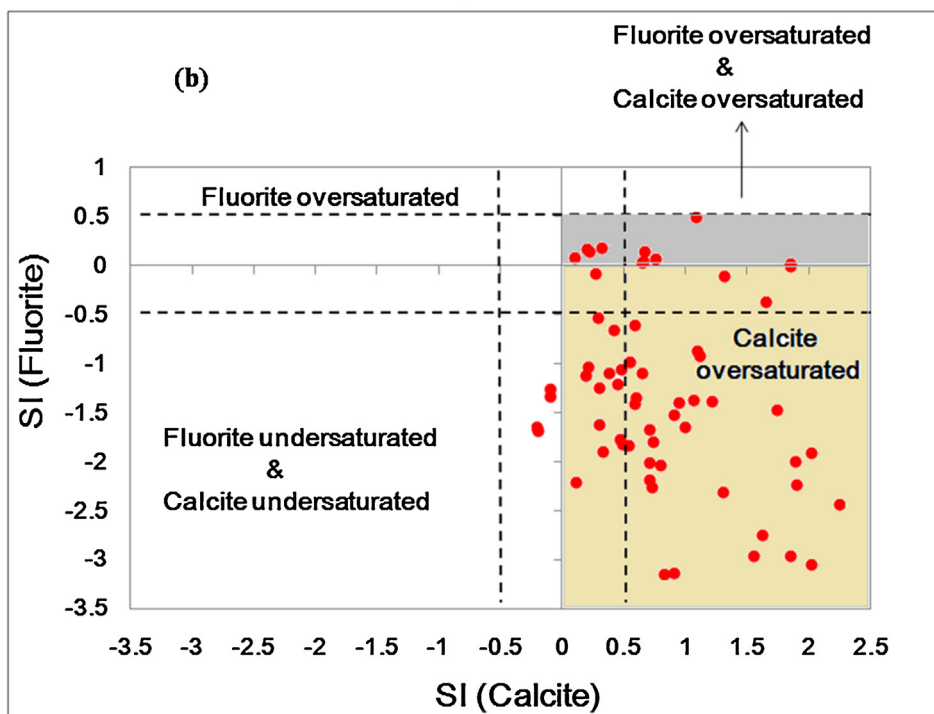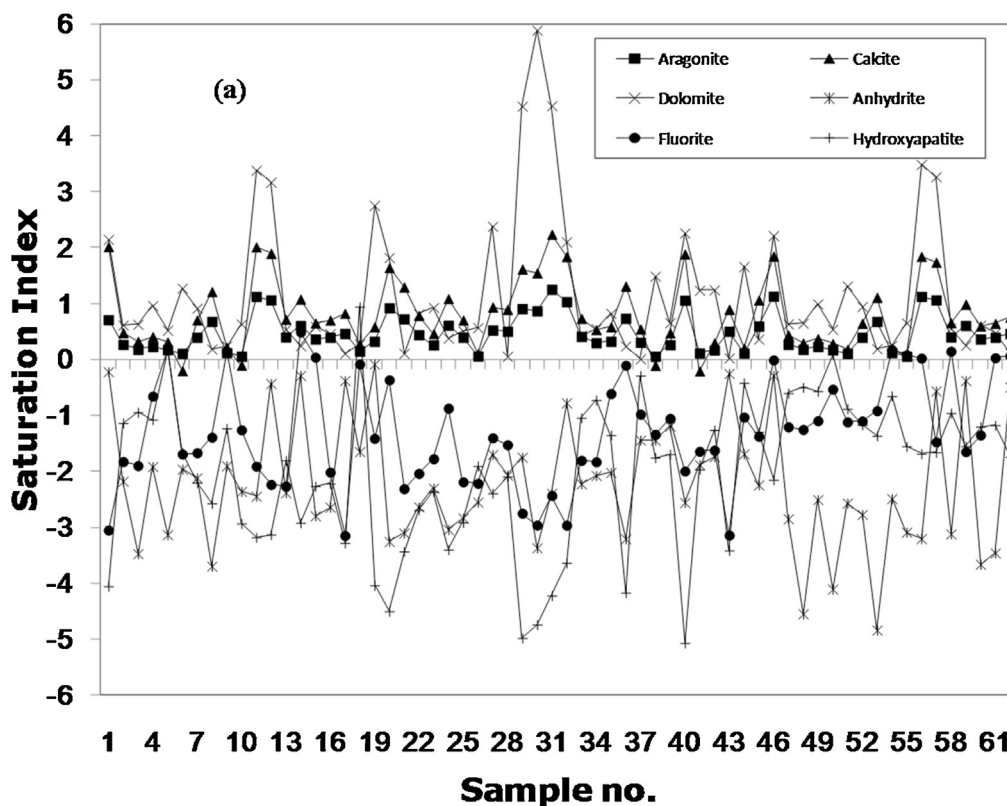
Fig. 4. Plot showing saturation indexes (a) minerals that relate to fluoride enrichment (b) SI (Fluorite) versus SI (Calcite) to elucidate the process responsible for fluoride enrichment.

Table 3
Multivariate statistical analysis with eigenvalues, % of variance, and cumulative variance.

Total variance explained

Component	Initial eigenvalues			Extraction sums of squared loadings			Rotation sums of squared loadings		
	Total	% of variance	Cumulative %	Total	% of variance	Cumulative %	Total	% of variance	Cumulative %
1	5.176	32.349	32.349	5.176	32.349	32.349	4.744	29.650	29.650
2	3.308	20.676	53.025	3.308	20.676	53.025	3.081	19.257	48.907
3	2.155	13.467	66.492	2.155	13.467	66.492	2.674	16.714	65.621
4	1.308	8.177	74.669	1.308	8.177	74.669	1.448	9.048	74.669
5	0.913	5.705	80.374						
6	0.723	4.517	84.891						
7	0.703	4.396	89.287						
8	0.496	3.102	92.389						
9	0.345	2.154	94.542						
10	0.310	1.938	96.480						
11	0.224	1.403	97.883						
12	0.184	1.149	99.032						
13	0.120	0.750	99.782						
14	0.033	0.209	99.991						
15	0.001	0.009	100.000						
16	0.000	0.000	100.000						

Table 4
Factor loadings for significant principal components (eigen values > 1).

	Component			
	1	2	3	4
pH	0.824	−0.180	−0.172	0.011
TDS	0.068	0.947	0.037	0.079
EC	−0.021	0.941	0.030	0.069
Alk	0.919	−0.019	0.064	−0.080
Acid	0.235	−.397	0.111	0.366
TH	0.398	−0.046	0.888	0.008
Ca	−0.587	0.154	0.672	0.084
Mg	−0.227	0.321	0.783	0.183
K	−0.287	0.059	0.318	0.603
Na	−0.454	0.534	0.206	−0.238
HCO3	0.919	−0.019	0.064	−0.080
Cl	0.708	0.486	0.337	−0.055
SO4	−0.506	0.593	0.151	−0.054
NO3	0.549	−0.180	0.676	−0.067
F	−0.639	0.268	−0.159	0.164
PO4	−0.068	0.010	−0.084	0.889

of chloride which is enriched due to high evaporation rate ultimately results in to salt patches, which leach out during the recharge process. Factor 3 shows higher positive loading of total hardness, Ca^{2+}, Mg^{2+} and NO_3^- (Table 4). It shows that mostly the factors responsible for hardness of water along with influence of nitrogenous fertilizers. Factor 4 shows higher positive loading for K^+, and PO_4^-, which again shows the impact of fertilizers used for agriculture (Table 4). First three PC loadings are plotted to observe the grouping and relationship among the variables. Plots of these three components explain 66.49% of total variance (Fig. 5). Component loading is used to analyze that how variables are correlated and which variable is most influential. Overall geochemical reactions controlling the F^- enrichment in groundwater in Patan district is also similar or well supported by the finding from Mehsana district located next to the study region (Dhiman and Keshari, 2006). This reveals that local mineralogical composition of the aquifer matrix is very much responsible for the localized F^- pollution.

5. Discussion

Relatively higher concentration of Na^+ might be contributed through rock water interaction i.e. weathering of rocks containing Na^+ (like schist, quartzite and granitic rocks abundantly present in the study area), cation-exchange (substitution of Na^+ and K^+ by Ca^{2+} and Mg^{2+} sorbed on the surface of clay) is mainly responsible for the dominance of Na^+ and Ca^{2+} in the groundwater samples (Srinivasamoorthy et al., 2008). The enrichment of Na^+ and Ca^{2+} in groundwater through feldspar weathering and cation exchange are shown in Eqs. (1) and (2) respectively:

$$NaAlSi_3O_8 + H_2CO_3 + H_2O \rightarrow Na^+ + HCO_3^- + 2H_4SiO_4 + 2Al_2Si_2O_5(OH)_4 \tag{1}$$

$$Na^+ + Ca - X_2 \rightarrow Ca^{2+} + Na - X \tag{2}$$

Here, for Eq. (2), Na^+ is adsorbed by the exchanger X while Ca^{2+} is released and Ca-HCO3 type water results.

Bicarbonate which is most dominant anion might be contributed through weathering of silicate rocks and decomposition of organic matter (Avtar et al., 2013). Relatively higher concentration of Cl^- in some samples (beyond WHO permissible limit of 600 mg/L) can be contributed by higher evaporation during recharge at spatial scale as well as input from sewage effluents (Kumar et al., 2015). Higher value of SO_4^{2-} and NO_3^- in few groundwater samples is mainly attributed to agriculture runoff as the study area has intense agriculture activity and breakdown of organic matter is prominent (Anderson, 1979). Concentration of F^- which is quite high in most of the groundwater samples is discussed in more detail in the next section to get an in-depth sight for geochemical processes responsible for its enrichment.
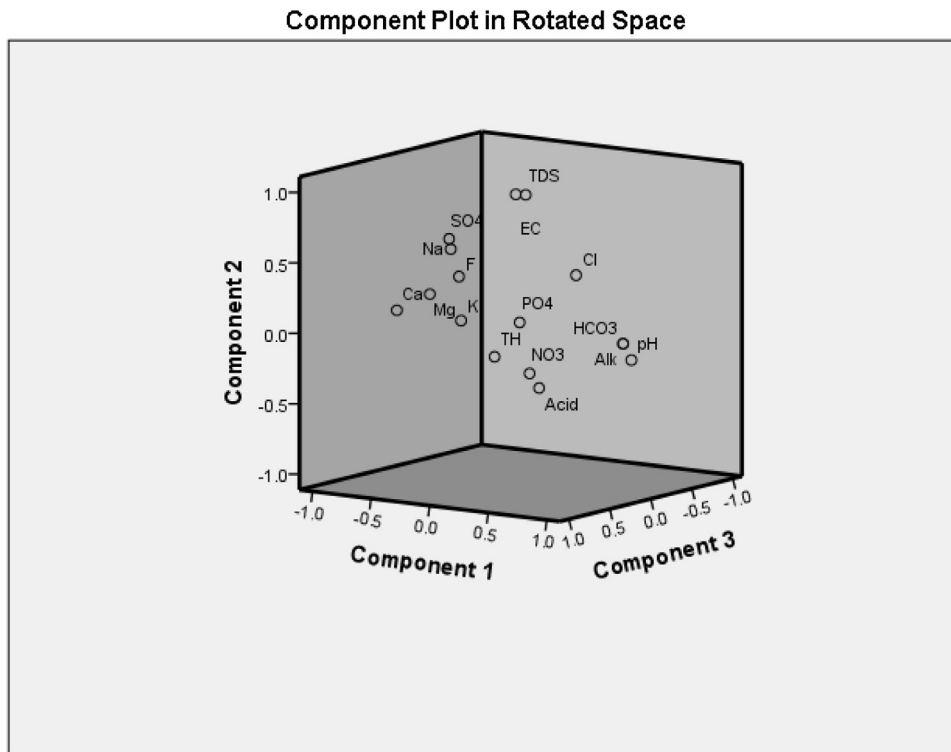
Fig. 5. Loadings of first three factors in 3-dimensional space showing correlation between water quality variables.

For F^- chemistry, generally in groundwater with pH < 7.0, F^- remains adsorbed to clay due to low solubility of F^-. However, in an alkaline medium, i.e. groundwater with pH > 7.0, OH^- group replaces the exchangeable F^- of clay minerals (biotite/muscovite) leading to an increase in the concentration of F^- in groundwater (Avtar et al., 2013; Singh and Mukherjee, 2014). Geochemically it is also known that F^- ions have the same charge and nearly the same radius as hydroxide ions, thereby, facilitating the replacement of each other. But concentration of F^- in groundwater also depends on the solubility of F^- bearing minerals, anion exchange capacity of aquifer materials (OH^- for F^-), the size and type of geological formations traversed by water, and the amount of time that water was in contact with a particular formation (Shanker et al., 2003). The possible reaction for replacement of F^- from OH^- ions in case of the muscovite is shown in Eq. (3).

$$KAl_2 \cdot [AlSi_3O_{10}] F_2 + 2OH^- \rightarrow KAl_2 \cdot [AlSi_3O_{10}] \cdot [OH_2] + 2F^- \tag{3}$$
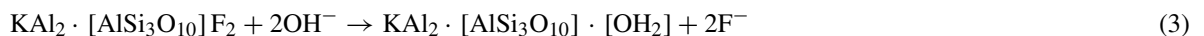
High correlation between F^- and alkalinity might be due to the release of OH^- and bicarbonate ions simultaneously during the leaching and dissolution process of F^- bearing minerals into groundwater. A higher rate of weathering and leaching of minerals also increases the F^- ion concentrations with higher levels of alkalinity. Another possibility is that the hydrolysis of alumino-silicate minerals in the hard rock aquifers produces bicarbonate ions, which can enhance fluorite dissolution. A possible reaction is shown in Eq. (4).

$$CaF_2 + 2HCO_3^- \rightarrow CaCO_3 + 2F^- + H_2O + CO_2 \tag{4}$$

Inverse relation between F^- and Ca can be attributed to precipitation of CaF_2 as carbonate, due to its lower saturation index or high solubility product (Gaciri and Davis, 1993; Gizaw, 1996).

Also poor correlation between F^- and nitrate divulges that apart from dissolved oxygen, nitrate is thermodynamically favored electron acceptor for providing reducing condition to enhance F^- mobilization ultimately results in its enrichment (Rose et al., 1979).

Most of the water contains Na-HCO_3 type of water facies, which also influences the dissolution of fluorite minerals and releases the F^- ions in groundwater (Li et al., 2012; Mrazovaca et al., 2013; Kumar and Singh, 2015).

Majority of hydrochemical facies clearly indicating dominant nature of Na^+, Ca^{2+} and HCO_3^- among all ionic species present in groundwater samples (Li et al., 2012; Mrazovaca et al., 2013; Kumar and Singh, 2015). Na-HCO$_3$ water type mainly depicts interaction of groundwater with granitic rocks containing minerals like schist and quartzite during its flow course. Ca-HCO$_3$ and Mg-HCO$_3$ water type is mainly from the rocks containing minerals like calcite, dolomite and gypsum. Whereas some of the water samples with Ca-Mg-SO$_4$-Cl nature clearly supports water quality alteration because of man-made activities.

From saturation index, oversaturation with respect to aragonite is supported by the fact that aragonite dissolution might be a subsidiary process operating at the study area along with the above mentioned reactions for the release of Ca^{2+} and HCO_3^- in groundwater. Oversaturation of these minerals reduces the concentrations of Ca^{2+} and Mg^{2+} in groundwater and indicates that calcite and dolomite are the dominant constituents of aquifer in the region. Groundwater of these aquifers has sufficient resident time to reach the equilibrium. Calcite precipitation in alkaline environment also favors dissolution of fluorite (Kumar and Singh, 2015).

On the other hand, under saturation with respect of fluorite might be just by alkaline medium of the groundwater system which is also well supported by a high rate of evaporation in semi-arid conditions, which might enhance calcite precipitation which removes Ca^{2+} from solution allowing more fluorite to dissolve. These released Ca^{2+} ions then combine with CO_3^{2-} ions to further enhance the precipitation of $CaCO_3$.

For factors analysis, first factor reveals the presence of high HCO_3^-, Na^+ and pH in the aquifer system favoring the release of F^- from aquifer matrix into groundwater. Second factor points towards high evaporation rate which is typical signature of semi-arid area resulting in high salt concentration and thus enrichment of Cl^-. Third and fourth factors emphasize the effect of agricultural practices affecting the groundwater chemistry.

6. Conclusion

F^- concentration in the groundwater samples of Patan districts ranges from 0.4 to 4.8 mg/L with an average value of 2.9 mg/L. Eighty percent of groundwater samples in the study area exceed the permissible limit of F^- concentration (1.5 mg/L) for drinking water supply. Some of the health related issues like dental fluorosis and skeletal fluorosis, leading to molting and pitting of teeth, stiffness and rigidity of joints were physically noticed during the time of sampling and medical examination is required to confirm the incidences due to consumption of F^- in groundwater. The result of the study points towards the geogenic source of F contamination of groundwater. The presence of high HCO_3^-, Na^+ and pH favors the release of F^- from the minerals such as fluorite into groundwater. The granite in the area contains abundant F^- and during weathering, F^- leaches out from the mineral phase into groundwater. Hydrogeochemical data suggests groundwater with high HCO_3^- and Na^+ ion concentrations in alkaline condition under the control of water–rock interactions coupled with climatic factors is the most primary–reason for the release of F^-. Geochemical modeling confirms the findings as most of the samples are undersaturated with respect to fluorite and oversaturated with respect to calcite thus creating a favorable environment for F release into groundwater. The calcite precipitation leads to the removal of Ca^{2+} from solution thus allowing more fluorite to dissolve. These released Ca^{2+} ions combine with CO_3^{2-} ions to further enhance the precipitation of $CaCO_3$. Finally it is concluded that F^- enrichment in groundwater is a cumulative effect of the mineral composition of rock present locally, alkaline conditions of the groundwater system regulated by processes such as rock–water interaction, ion-exchange and evaporation.

References

Ando, M., Tadano, M., Yamamoto, S., Tamura, K., Asanuma, S., Watanabe, T., 2001. Health effects of fluoride pollution caused by coal burning. Sci. Total Environ. 271, 107–116.

Avtar, R., Kumar, P., Surjan, A., Gupta, L.N., Roychowdhury, K., 2013. Geochemical processes regulating groundwater chemistry with special reference to nitrate and fluoride enrichment in Chhatarpur area Madhya Pradesh, India. Environ. Earth Sci. 70, 1699–1708.

Boyle, D.R., Chagnon, M., 1995. An incidence of skeletal fluorosis associated with groundwater of the maritime carboniferous basin, Gaspé region, Quebec, Canada. Environ. Geochem. Health 17, 5–12.

CGWB (Central Ground Water Board), Ministry of water resources, Government of India (2010). Ground water quality in shallow aquifers of India, pp. 233.

Cao, J., Zhao, Y., Lin, J.W., Xiao, R.D., Danzeng, S.B., 2000. Environmental fluoride in Tibet. Environ. Res. 83, 333–337.

Carrillo-Rivera, J.J., Cardona, A., Edmunds, W.M., 2002. Use of abstraction regime and knowledge of hydrogeological conditions to control high fluoride concentration in abstracted groundwater San Luis Potosy basin, Mexico. Hydrogeol. J. 261, 24–47.

Coetsiers, M., Walraevens, K., 2006. Chemical characterization of the neogene aquifer, Belgium. Hydrogeol. J. 14, 1556–1568.

Dhiman, S.D., Keshari, A.K., 2006. Hydrogeochemical evaluation of high-fluoride groundwaters: a case study from Mehsana District, Gujarat, India. Hydrol. Sci. 51 (6), 1149–1162.

Gaciri, S.J., Davis, T.C., 1993. The occurrence and geochemistry of fluoride in some natural waters of Kenya. J. Hydrol. 143, 395–412.

Garrels, R.M., Mackenzie, F.T., 1971. Evolution of Sedimentary Rocks. Norton and Company, New York, pp. 394.

Gizaw, B., 1996. The origin of high bicarbonate and fluoride concentration in waters of the main Ethiopian rift valley, East African rift system. J. Afr. Earth Sci. 22, 391–402.

Goldman, S.M., Sievers, M.L., Templin, D.W., 1991. Radiculomyopathy in a southwestern Indian due to skeletal fluorosis. Ariz. Med. 28, 675–677.

Huh, Y., Tsoi, M.Y., Zaitiser, A., Edward, J.N., 1998. The fluvial geochemistry of the river of Eastern Siberia. I. Tributaries of Lena River draining the sedimentation platform of the Siberia Craton. Geochim. Cosmochim. Acta 62, 1657–1676.

Hussain, I., Arif, M., Hussain, J., 2012. Fluoride contamination in drinking water in rural habitations of Central Rajasthan, India. Environ. Monit. Assess. 184, 5151–5158.

IPCS, 1984. Fluorine and fluorides. Geneva, World Health Organization, International Programme on Chemical Safety (Environmental Health Criteria 36), pp. 180.

Jacks, G., Bhattacharya, P., Chaudhary, V., Singh, K.P., 2005. Controls on the genesis of some high-fluoride groundwaters in India. Appl. Geochem. 20, 221–228.

Johnson, A., Abbaspour, K., Amini, M., Bader, H.P., Berg, M., et al., 2008. Geogenic contaminants. Research Reports, Eawag News 65e/December, 16–19.

Keshari, A.K., Dhiman, S.D., 2001. Genesis of fluoride contamination in the Western Indian Aquifers. In: Future Groundwater Resources at Risk Proceeding of Third International Conference, Lisbon, Portugal, 25–27 June 2001, Theme 3: Point and non-point source pollution, pp. 1–8.

Kharb, P., Susheela, A.K., 1994. Fluoride ingestion in excess and its effect on organic and certain inorganic constituents of soft tissues. Med. Sci. Res. 22, 43–44.

Kumar, P., Kumar, M., Ramanathan, A.L., Tsujimura, M., 2010. Tracing the factors responsible for arsenic enrichment in groundwater of the middle Gangetic Plain, India: a source identification perspective. Environ. Geochem. Health 32, 129–146.

Kumar, P., Kumar, A., Singh, C.K., et al., 2015. Hydrogeochemical Evolution and Appraisal of Groundwater Quality in Panna District, Central India. Expo Health 8 (1), 19–30.

Kumar, A., Singh, C.K., 2015. Characterization of hydrogeochemical processes and fluoride enrichment in groundwater of South-Western Punjab. Water Qual. Expo. Health, 1–15.

Leung, D., Hrudey, S.F., 1985. Removal of fluorides from water supplies. Alberta Environmental Standard and Approval Division, July 1985, pp. 107.

Liu, C.W., Lin, K.H., Kuo, Y.M., 2003. Application of factor analysis in the assessment of groundwater quality in black foot disease in Taiwan. Sci. Total Environ. 313, 77–89.

Madhavan, N., Subramanian, V., 2002. The natural abundance of fluoride in soils of the Ajmer distict, Rajasthan. J. Environ. Monit. 4, 821–822.

Meenakshi, Maheshwari, R.C., 2006. Fluoride in drinking water and its removal. J. Hazard. Mater. 37, 456–463.

Mondal, N.C., Prasad, R.K., Saxena, V.K., Singh, Y., Singh, V.S., 2009. Appraisal of highly fluoride zones in groundwater of Kurmapalli watershed, Nalgonda district, Andhra Pradesh (India). Environ. Earth Sci. 59, 63–73.

Parkhurst, D.L., Appelo, C.A.J., 1999. User's Guide to PHREEQC (Version 2)—A Computer Program for Speciation, Batch-Reaction, One-Dimensional Transport, and Inverse Geochemical Calculations. United States Geological Survey, Water Resources Investigations Report 99-4259, Washington, DC, pp. 326.

Ranjan, R.K., Ramanathan, A.L., Parthasarathy, P., Kumar, A., 2013. Hydrochemical characteristics of groundwater in the plains of Phalgu River in Gaya, Bihar, India. Arab. J. Geosci. 6 (9), 3257–3267.

Rose, A.W., Hawkes, H.E., Webb, J.S., 1979. Geochemistry in Mineral Exploration, 2nd edn. Academic Press, London, pp. 657.

Shaji, E., Bindu, V.J., Thambi, D.S., 2007. High fluoride in groundwater of Palghat District, Kerala. Curr. Sci. 92, 240–245.

Shanker, R., Thussu, J.L., Prasad, J.M., 2003. Geothermal studies at Tattapani hot spring area, Sarguja district, central India. Geothermics 16, 61–76.

Singh, C.K., Mukherjee, S., 2014. Aqueous geochemistry of fluoride enriched groundwater in arid part of Western India. Environ. Sci. Pollut. Res. 22 (4), 2668–2678.

Singh, C.K., Kumari, R., Singh, N., Mallick, J., Mukherjee, S., 2012. Fluoride enrichment in aquifers of the Thar Desert: controlling factors and its geochemical modeling. Hydrol. Process. 27, 2462–2474.

Singh, C.K., Kumari, R., Singh, R.P., Shashtri, S., Kamal, V., Mukherjee, S., 2011a. Geochemical modeling of high fluoride concentration in groundwater of Pokharan area of Rajasthan, India. Bull. Environ. Contam. Toxicol. 86, 152–158.

Singh, C.K., Shashtri, S., Mukherjee, S., 2011b. Integrating multivariate statistical analysis with GIS for geochemical assessment of groundwater quality in Shiwaliks of Punjab, India. Environ. Earth Sci. 62 (7), 1387–1405.

Srinivasamoorthy, K., Chidambaram, S., Prasanna, M.V., Vasanthavihar, M., Peter, J., Anandhan, P., 2008. Identification of major sources controlling groundwater chemistry from a hard rock terrain—a case study from Mettur taluk, Salem district, Tamil Nadu, India. J. Earth Syst. Sci. 117 (1), 49–58.

UNDP/CGWB (United Nations Development Programme/Central Ground Water Board), 1976. Groundwater surveys in Rajasthan and Gujarat, India, Tech. Report, United Nations.

UNICEF, 2008. UNICEF Handbook on Water Quality. United Nations Children's Fund, New York.

WHO, 1993. Guidelines for Drinking Water Quality: Recommendation, vols. 1–2. World Health Organization, Geneva, 188 p.